

2018

Enrichment of surface ice stable water isotope ratios following sublimation

<https://hdl.handle.net/2144/33056>

"Downloaded from OpenBU. Boston University's institutional repository."

BOSTON UNIVERSITY
GRADUATE SCHOOL OF ARTS AND SCIENCES

Thesis

**ENRICHMENT OF SURFACE ICE STABLE WATER
ISOTOPE RATIOS FOLLOWING SUBLIMATION**

by

DONOVAN PATRICK DENNIS

B.A., Occidental College, 2016

Submitted in partial fulfillment of the
requirements for the degree of
Master of Arts

2018

© 2018 by
DONOVAN PATRICK DENNIS
All rights reserved

Approved by

First Reader

Andrew C. Kurtz, PhD
Professor of Earth and Environment

Second Reader

Mark A. Friedl, PhD
Professor of Earth and Environment

Third Reader

John M. Fegyveresi, PhD
Adjunct Assistant Professor of Earth and Environment

Fourth Reader

Dirk Scherler, PhD
Junior Professor
Deutsches GeoForschungsZentrum and Freie Universität Berlin

*All there is to thinking is seeing something noticeable
which makes you see something you weren't noticing
which makes you see something that isn't even visible.*

- Norman Maclean, *A River Runs Through It and Other Stories*

Acknowledgments

Financial support for this project was partially provided through funds granted to Dr. David Marchant by the Howard Hughes Medical Institute Professors Program. Additional support was provided by the BU Dept. of Earth and Environment.

First, I extend my gratitude to Prof. Marchant for the opportunities he provided during my time at BU. I am also very grateful for the guidance of Andy Kurtz, who reviewed numerous drafts of this manuscript and helped guide it to completion. My additional committee members—Mark Friedl, John Fegyveresi, and Dirk Scherler—provided helpful comments and suggestions that improved this text, for which I am most appreciative. Many thanks to Joel Sparks, too; his aptitude for experimental design was an essential component of this work.

For her assistance in surmounting administrative obstacles and her unwavering support, I am indebted to Alissa Beideck, whose patient counseling will forever be appreciated.

I am additionally grateful for our undergraduate researchers, Olivia Williams and Shuhui Liu, who provided assistance when requested and, more importantly, did not allow my manic anguish during the development of our experimental design to deter them from Earth science.

To my colleague and friend, Shivani Ehrenfeucht: I am thankful beyond words to have had such an understanding and clear-headed confidant during these challenging months. Your kindness, thoughtfulness, and honesty are eclipsed only by your intelligence, and I am both a better person and scientist because of our friendship. I cannot wait to someday tell people that I know you.

And finally, I wish to thank my friends and my family at home in Montana for their unceasing support of my continued education. Particularly my parents, Teresa and David, my siblings, my late grandparents Russell and Linaire, and my cousin, Sarah, who always insists that I achieve my potential.

To the aforementioned and the many others who have aided me along the way, my heartfelt thanks.

Cincin.

**SURFACE ENRICHMENT OF STABLE ISOTOPE RATIOS IN ICE
BY SUBLIMATION**

DONOVAN PATRICK DENNIS

ABSTRACT

Stable isotopes of water preserved in glaciers and icesheets have revolutionized our understanding of terrestrial paleoclimate. Post-deposition alteration of the stable water isotope ratios in snow and ice can obscure the original meteoric signal, therefore altering the interpretation of $\delta^{18}\text{O}$ and δD as records of paleo-temperatures in ice. The effects of sublimation on $\delta^{18}\text{O}$ and δD are not well-understood for massive (non-snow) ice and have been largely overlooked, particularly within the experimental literature. We present results from a series of environmental chamber experiments investigating alteration of the in-situ signal following sublimation. Our data suggest that sublimation enriches the ice remaining after sublimation in ^{18}O and D. This is observed both in surface ice and in the signal of the ice at depth. These results could have important implications for studies utilizing surface ice $\delta^{18}\text{O}$ and δD for reconstructions of paleoclimate.

Contents

1	INTRODUCTION	1
1.1	Theoretical Background	1
1.2	Brief Review of the Applied Literature	4
2	EXPERIMENTAL METHODS	8
2.1	Ice Column Freezing Methods	8
2.2	Sublimation Experiments	11
2.2.1	Sublimation-maximized experiment	12
2.2.2	Surface till sublimation experiment	13
3	EXPERIMENTAL RESULTS	15
4	DISCUSSION	19
4.1	Evidence for sublimation-induced fractionation	19
4.1.1	Pre-sublimation and post-sublimation surface δD values	19
4.1.2	Comparison of the meteoric, freezing and sublimation water line slopes	21
4.1.3	Mass balance of the post-sublimation columns	22
4.2	Proposed mechanism for alteration at depth	24
4.3	Implications for paleoclimate reconstructions using surface-exposed ice	25
4.4	Study limitations and future directions	27
5	CONCLUSIONS	30
A	APPENDIX: ALL DATA	31
	References	35
	Curriculum Vitae	40

List of Tables

1	Summary of core names for each experiment.	15
2	Summary data for Experiment 1, the initial sublimation experiment designed to maximize ice sublimation. Columns were left to sublimate at -2 °C and 20 % relative humidity for 20 days.	18
3	Summary data for Experiment 2, the sublimation experiment with a mimicked surface “debris” of glass beads. Columns were left to sublimate at -10 °C and 20 % relative humidity for 19 days. Column 4-9 was omitted from analysis due to errors during sampling.	19
4	Break point depths for sublimated ice columns. Break points were calculated using the R statistical software ‘segmented’ package (Muggeo, 2008).	19
5	Vapor and bulk liquid δD calculated using fractionation factors (α) reported in the experimental literature. The measured bulk water value is -56.6 ‰. Due to the variability in the reported α -values, we observe a 10‰ range in our calculated vapor δD . This variability is not present in the calculated bulk water values because much less material sublimated off compared to the amount that remained in the solid phase.	23

List of Figures

1	Schematic diagrams for the (a) freezing development methods; (b) sublimation-maximized experiment; and (c) surface debris experiment.	9
2	Exaggerated freezing pattern schematic (a) and the modeled evolution of $\delta^{18}\text{O}$ in ice column 2-A (b). Figure 2b employs a freezing boundary layer of 0.015 cm, freezing rate of 1.7 cm hr^{-1} and a diffusivity of ^{18}O in liquid water of $1.1 \times 10^{-5} \text{ cm}^2 \text{ sec}^{-1}$ following Lacelle et al. 2011. We believe the boundary layer to have been minimal at the onset of freezing due to vigorous mixing by the stir bar. Because the stir bar was immobilized during freezing, however, neither the boundary layer thickness nor the freezing rate were likely constant through time. Two different alpha values are used, 1.0031 and 1.0028, which correspond to the respective evolution curves. Samples from ice column 2-A are plotted along the curves.	11
3	Depth profiles of δD , $\delta^{18}\text{O}$, and D-excess for the non-sublimated ice columns.	16
5	Plots of δD against $\delta^{18}\text{O}$ for all samples. The regression lines plotted are analogous to meteoric water lines (MWL). Here they are termed the “freezing water line” (FWL) and “sublimation water line” (SWL); see section 4.1 Evidence for sublimation-induced fractionation.	17
4	Depth profiles of δD , $\delta^{18}\text{O}$, and D-excess for the sublimated ice columns. Of note are the surface trends which suggest enrichment of the heavy isotope and a decrease in D-excess.	17

6	Theoretical schematic illustrating the effect of sublimation on isotope abundances at the ice surface. As the surface is enriched in the heavy isotopologues, the heavier molecules diffuse downwards away from the sublimation front. Thin liquid films described by Nye et al. [1998] facilitate the diffusion of these heavier isotopologues more quickly than would be anticipated via solid-state diffusion.	26
---	---	----

1 INTRODUCTION

The analysis of stable water isotopes has, over the past half-century, led to exceptional discoveries in the Earth and planetary sciences. Their utility as a proxy for terrestrial paleoclimate has expanded beyond the Earth's cryosphere, and stable hydrogen and oxygen isotopes are studied in a variety of materials to better understand both present and past global change. Improved analytic capacities developed in recent decades have additionally allowed for expanded study in both field and laboratory settings. As measurement precision increases, so too does the ability to study processes occurring at smaller scales and with lower magnitude effects. One of these processes, sublimation-induced fractionation of glacier ice in close proximity to the atmosphere, has received little attention in the experimental literature. This project therefore sought to understand what effect, if any, sublimation has on the stable isotope ratios of ice. We first review the fundamental principles that govern fractionation during changes of phase and the application of this work both in experimental and field studies. We then report and describe results from a series of environmental chamber experiments investigating the effects of sublimation on the stable water isotope values of surface, sub-surface, and debris-overlain ice. This work is particularly relevant for stable isotope investigations of massive ground and glacial ice exposed to the atmosphere and/or subjected to prolonged periods of sublimation. The findings of this investigation will additionally contribute to the broader understanding of the effects of sublimation on firn and ice.

1.1 Theoretical Background

The use of hydrogen and oxygen isotopes as a proxy for paleo-temperature is rooted in the physics of fractionation. Fractionation, the partitioning of heavy and light isotopes into the solid, liquid, or vapor states, occurs during all phase change reactions, and is broadly defined to include both kinetic fractionation and equilibrium fractionation. Isotope abundances are reported as a normalized ratio of the concentration of the

heavy isotope to the concentration of the light isotope, calculated as

$$\delta D = \left(\frac{\left(\frac{D}{H}\right)_{sample}}{\left(\frac{D}{H}\right)_{standard}} - 1 \right) * 1000 , \quad (1)$$

using the δ calculation for Deuterium (D) as an example.

Equilibrium fractionation in water¹ is dictated by the molecules’ zero-point energies, a measure of the bond strength between atoms. Bond strength is mass-dependent, therefore isotopologues with higher mass atoms (heavy isotopes) have stronger bonds than isotopologues absent heavy atoms. As the molecules of water transition between phases, the isotope ratios in either phase can be predicted by the fractionation factor (α), a temperature-dependent constant, defined as

$$\alpha = \frac{\left(\frac{D}{H}\right)_{Phase A}}{\left(\frac{D}{H}\right)_{Phase B}} . \quad (2)$$

For temperatures above -50 °C, α -values are inversely correlated with temperature—therefore the lower the temperature the greater the α -value and the more exaggerated the difference between the vapor and the remaining ice reservoir (Merlivat and Nief, 1967; Lécuyer et al., 2017). The α -values for all phase changes have been reported extensively both in the theoretical and experimental literature. Due to the instrumental limitations of recreating perfectly-equilibrium conditions within a laboratory setting, studies have yielded small variations in experimentally-derived α -values for given temperatures. The determination of these values therefore remains a subject of active research. See Merlivat and Nief (1967), Lécuyer et al. (2017), and Ellehoj et al. (2013) for a thorough review of the fractionation factors for sublimation. As small deviations in α -values lead to considerable differences in modeled δ -values, we use a suite of literature-reported fractionation factors for our calculations within, as indicated in the Experimental Results and Discussion sections.

A second fractionation mechanism, kinetic or “transport” fractionation, is a

¹Throughout this text “water” will refer to the compound H₂O and water in the liquid phase will be referred to as “liquid.”

function of the diffusivity of water isotopologues in air, liquids, and solids. Kinetic fractionation is commonly observed in unidirectional processes and serves to amplify the effects of equilibrium fractionation. It is most pronounced in open systems within which the continuous removal of material drives unidirectional fractionation and sequestration of isotopes into their respective stable phases. Kinetic/transport fractionation therefore combines the effects of equilibrium fractionation, mass-dependent diffusion, and the unique chemical properties of water (Gat, 2010).

In natural systems, equilibrium and kinetic fractionation of water is driven by environmental conditions like temperature and, to a lesser extent, humidity (Merlivat and Jouzel, 1979; Dansgaard, 1964). These conditions are therefore tied to δ -values which reflect the net fractionation of the water. High-energy systems will more readily evaporate the heavy isotopologue of water as compared to low-energy systems. The δ -values for vapor evaporated in a high-energy (i.e. warmer) system will therefore be “enriched” in the heavy isotope compared to the “depleted” low-energy system. This important link between temperature and net isotope fractionation is the relationship that allows for the use of stable water isotope ratios as a proxy for temperature.

When δD is plotted as a function of $\delta^{18}O$, the slope of the linear regression line relating these two values is a function of the phase change-induced fractionation the material has undergone. The δD - $\delta^{18}O$ regression line of precipitated water in the hydrologic cycle is referred to as a “meteoric water line.” The global meteoric water line (GMWL) relates the abundance of ^{18}O and D species in precipitation averaged for global waters, and is defined as

$$\delta D = 8 * \delta^{18}O + 10 \quad (3)$$

Because ^{18}O and ^{16}O have a larger mass difference than D and H, the magnitude of fractionation during phase changes is not uniform between the two elements. The different phase changes can therefore be identified via the slope of the δD - $\delta^{18}O$ regression line of given water samples. The slope of the δD - $\delta^{18}O$ regression line for

ice subjected to sublimation is expected to be between 4 and 6 (Lacelle et al., 2013; Sokratov and Golubev, 2009). Liquid reservoirs subjected to evaporation commonly yield slopes between 2 and 5 (Clark and Fritz, 1997; Kim and Lee, 2011), and the slope of water subjected to freezing generally falls between 6 and 7.5, though has been observed as low as 4.37 depending on the source water δ -values (Merlivat and Nief, 1967; Lacelle, 2011; O’Neil, 1968; Matsuoka, 1999).

The “excess” D relative to ^{18}O and the global meteoric water line is commonly used in isotope hydrology as a proxy for vapor source region and humidity. It is calculated as

$$\text{D-excess } (d) = \delta\text{D} - 8 * \delta^{18}\text{O} . \quad (4)$$

and referred to as “D-excess” (d). It can similarly be used to identify alternative processes.

The phase transitions important to this study are freezing and sublimation, both of which have corresponding fractionation factors, as discussed above. It is useful to note that the general “phase favorability” for heavy isotopes can be described as solid > liquid > vapor, where the solid phase is the most favorable and therefore most likely to have an abundance of heavy isotope, and the vapor phase the least favorable.

1.2 Brief Review of the Applied Literature

As noted above, fractionation-controlled isotope abundances in all phases represented in the hydrologic cycle have important applications in the study of global climate, both past and present. Utilizing the link between δ -values and temperature, analysis of ancient precipitation preserved in glacial ice has allowed for reconstructions of global temperatures for the past $\sim 800,000$ years (EPICA Community Members, 2004). These reconstructions, however, rely upon a number of assumptions, including a constant linear relationship between temperature and precipitation isotopic composition through time and across space (Jouzel et al., 1997). Recently, considerable effort has been

devoted to studying the alteration of the isotope concentrations of snow during metamorphism and firnification but before their eventual preservation as glacial ice (Ellehoj et al., 2013; Ekaykin et al., 2009; Schotterer et al., 2004; Stichler and Schotterer, 2000; Town et al., 2008). These alternative post-deposition processes can include macro-scale mass transfer and kinetic fractionation effects via evaporation, wind scouring, melt/refreeze, rain percolation, and sublimation, in addition to closed-system snow and firnpack isotope diffusion. Schotterer et al. (2004) and Town et al. (2008) each provide a comprehensive overview of these effects and their respective magnitudes.

In both experimental and field studies, sublimation has been shown to enrich residual snow and firn in the heavy isotope species (Hoshina et al., 2014; Neumann et al., 2009; Sokratov and Golubev, 2009; Stichler et al., 2001; Ebner et al., 2017). Within the experimental literature, numerous studies of snow indicate a demonstrable alteration due to sublimation (Neumann et al., 2009; Sokratov and Golubev, 2009), termed “ventilation” by many to refer to the movement of vapor from snow pore spaces into the atmosphere (Casado et al., 2016; Town et al., 2008). These studies complement the theoretical and modeling literature which additionally predict fractionation due to sublimation (Jouzel et al., 1997; Merlivat and Nief, 1967). In field studies, however, the magnitude of alteration is complicated by environmental conditions, notably variable accumulation rates. At sites with low accumulation, like the South Pole, fractionation effects due to sublimation are amplified whereas in areas of high accumulation the alteration is muted by the continuous addition of snow and the ever-increasing height of the diffusive gradient between snow once at the surface and the atmosphere (Hoshina et al., 2014). Additionally, as firn is more dense than snow, it is anticipated that sublimation would have a more muted effect, though the relationship between depth, density, and magnitude of alteration for firn absent a snow-cover buffer is not well-constrained either by the field or experimental literature (Stichler et al., 2001).

Unlike snow and firn, however, it has previously been asserted that isotopic

fractionation due to sublimation has negligible effects on the stable water isotope record of solid glacier ice (Dansgaard, 1964; Dansgaard et al., 1973; Friedman et al., 1991). The low self-diffusion coefficient of individual water molecules within ice grains (Ramseier, 1967) justifies this assumption, as limited diffusion inhibits internal exchange and reorganization of molecules in the ice crystal matrix (Ekaykin et al., 2009).

Observations of GRIP ice core stable isotope data suggest, however, that diffusivity within in-situ ice can be nearly an order of magnitude higher than predicted by the theoretical diffusivity coefficient of Ramseier (1967) (Johnsen et al., 2000). Investigation of the GRIP core ice matrix revealed that liquid water exists within polycrystalline ice at films on grain boundaries, at grain triple junctions, and in melt figures, which facilitate diffusion within the ice (Nye, 1998; Mader, 1992; Rempel et al., 2001). The liquid is present both as a function of the structure of the ice matrix, and as the result of impurities within the ice. Importantly, the liquid is in equilibrium with the ice (Mader, 1992), suggesting that any fractionation between the solid and liquid phase would be likely dictated by the fractionation factor (α).

Lacelle et al. (2011) employ the interconnected microfilms diffusion mechanism proposed by Johnsen et al. (2000) to explain an observed alteration due to sublimation in buried massive ice from University Valley, Antarctica. As ^{16}O and H preferentially sublime from the surface of the ice, the uppermost layer is subsequently enriched in the heavy isotope. This induces Fickian diffusion into the ice at depth as the concentration of heavy isotopes is greater at the surface than below (Lacelle, 2011). The interconnected liquid microfilms facilitate diffusion and subsequent alteration of the ice at depth. The net sublimation-diffusion effect is characterized by both a sharp enrichment in the heavy isotope abundance and a decrease in D-excess (d) at the surface (Lacelle et al., 2013; Fisher and Lacelle, 2014), mimicking a sublimation fingerprint observed in Quelccaya icecap firn (Stichler et al., 2001).

Attributing the trends in University Valley ice to sublimation is additionally

supported by the limited experimental literature. Sokratov and Golubev (2009) sublimated shallow Petri dishes of ice at $-4\text{ }^{\circ}\text{C}$ and observed 1-2 ‰ enrichment in $\delta^{18}\text{O}$ and 4-8 ‰ enrichment in δD for surface ice. Observations of sublimating vapor in a vacuum by Brown et al. (2012) suggest similarly that fractionation of heavy isotope species occurs during sublimation with a measurable effect on the vapor generated (Brown et al., 2012). These findings suggest a previously untested, though potentially non-trivial, effect of sublimation on stable water isotope abundances in surface and shallow sub-surface ice. Until now, no experimental study has reported on alteration of the ice stable isotope signal at depth following sublimation in a controlled laboratory setting.

2 EXPERIMENTAL METHODS

2.1 Ice Column Freezing Methods

Prior to the sublimation experiments, we developed a standardized freezing method for production of experimental ice columns. Approximately 6.5 liters of Poland Spring brand filtered water were poured into two 6-in. (15.24 cm) diameter PVC tubes. All water came from the same well-mixed container.² To minimize potential evaporation and communication between the liquid and the ambient air during freezing, the cylinder tops were capped and a 0.125 in. (0.32 cm) diameter hole was drilled in the cap to alleviate pressure buildup due to ice volume expansion during freezing. We chose to use PVC with removable lids rather than manufactured or machined canisters to allow for easier removal of the ice from the container post-freezing. The plastic tubes were wrapped in <1 cm-thick plastic shipping wrap to insulate the containers and shield the ice columns from slight perturbations in ambient chamber temperature.

Previous field and laboratory experiments by others suggest the magnitude of the sublimation effect is variable and was believed to be small (Sokratov and Golubev, 2009; Stichler et al., 2001). We therefore sought a homogenous distribution of the heavy isotope species within the ice column, minimizing the fractionation signal imparted during freezing. This would ideally allow for clearly-defined alteration effects observed following sublimation. To achieve this homogeneity, the liquid was mixed during freezing by an unheated stir plate and 2.5 in. (6.35 cm) magnetic stir bar (Fig. 1) which reduced the width of the depleted boundary layer commonly found adjacent to the freezing front of the ice (Lehmann and Siegenthaler, 1991; Lacelle et al., 2013). We chose to use a stir plate for mixing the liquid as it allowed for the easy removal of the stirring apparatus after freezing and before sublimation, thereby not affecting the sublimation experiments, unlike vertical rod stirrers.

We additionally sought to minimize the column freezing time, which would again

²For more information about the water used, including sources and filtration, see (Nestlé Waters North America, 2016)

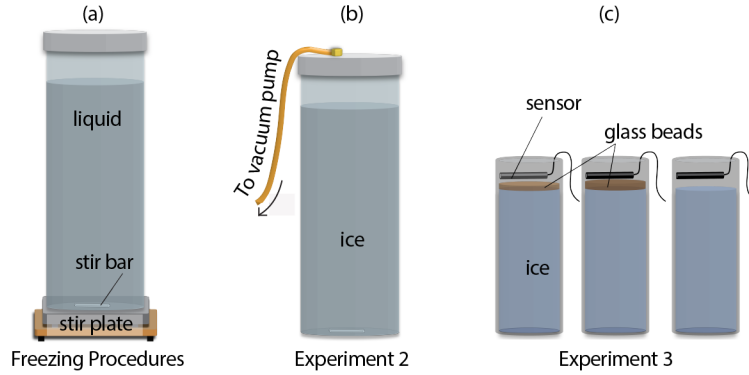


Figure 1: Schematic diagrams for the (a) freezing development methods; (b) sublimation-maximized experiment; and (c) surface debris experiment.

reduce fractionation during freezing. However, as super-cooled and rapidly-frozen ice can often result in intra-matrix cracks (Uyeda and Kikuchi, 1978) that could affect internal diffusion during sublimation (Johnsen et al., 2000; Brown et al., 2012), we used a step-freezing method. The cylinder filled with liquid water was placed in a freezer set to $+1$ °C and cooled overnight. Following cooling, the liquid was sampled and placed in an ESPEC Platinous Continuous Series environmental chamber and frozen step-wise, cooling -1 °C every three minutes to a minimum temperature of -50 °C. The water remained at -50 °C until frozen (~ 8 hours) and then was brought to $+10$ °C again at $+1$ °C intervals every three minutes. This generally, though not always, prevented post-freezing cracking within the ice matrix.

As noted above, consideration was given to the following desired specifications during freezing methods development: (1) a crack-free ice column; (2) ease of removal from container; (3) ability to continuously mix the liquid during freezing; and (4) rapid freezing time. Following freezing, the ice columns were removed from the chamber, halved using a table saw, and each half sampled using a 0.75 in. (1.91 cm) diameter hole saw. Sampling with the hole saw achieved ~ 2 cm sampling resolution down the center of the column. In addition to the center of the ice column, we additionally sampled the column edges to determine any edge effects. The ice was processed and melted internally at Boston University before shipment to the Iowa State University

Department of Geological and Atmospheric Science Stable Isotope Lab for δD and $\delta^{18}\text{O}$ analysis. Samples were measured using a Picarro L2130-i Isotopic Liquid Water Analyzer with autosampler and ChemCorrect software. Each sample was measured a total of six times. To account for memory effects, only the last three injections were used to calculate mean isotopic values. Reference standards (USGS 48, USGS 47) were used for regression-based isotopic corrections and to assign the data to the appropriate isotopic scale. At least one reference standard was used for every five samples. The analytic uncertainty for $\delta^{18}\text{O}$ is ± 0.06 ‰ (VSMOW) and δD is ± 0.29 ‰ (VSMOW), respectively.

After numerous trials, we could not successfully create an isotopically-homogeneous ice column that met the above specifications, a function of both the large volume of water and the eventual immobilization of the stir bar during freezing. Despite this, we determined the resultant non-homogeneous ice to be satisfactory for the sublimation experiments as the δ -trend of the innermost ice was very-nearly consistent (Fig. 3). Modeled liquid and solid evolution during freezing suggest a distinct freezing pattern; this is confirmed by visual observations during the course of freezing. The top of the column froze first, followed shortly thereafter by the exterior edges. The bottom of the column was the last exterior surface to freeze due to both the vigorous action of the stir bar and the bottom edge's slight insulation from the chamber air due to its contact with the stir plate. The freezing pattern and pre-sublimation ice column $\delta^{18}\text{O}$ and δD profiles are shown in Figs. 2a and 3. We note the obvious edge effect and the effect of fractionation during freezing imposed on the ice column. Additionally, we identified two visually-apparent "facies" in the ice: clear outer ice and slightly more opaque inner-column ice. It is important to note that in subsequent experiments the ice alternated between freezing bottom-up and top-down. The freezing pattern can be ascertained regardless using liquid/solid evolution curves (Fig. 2b).

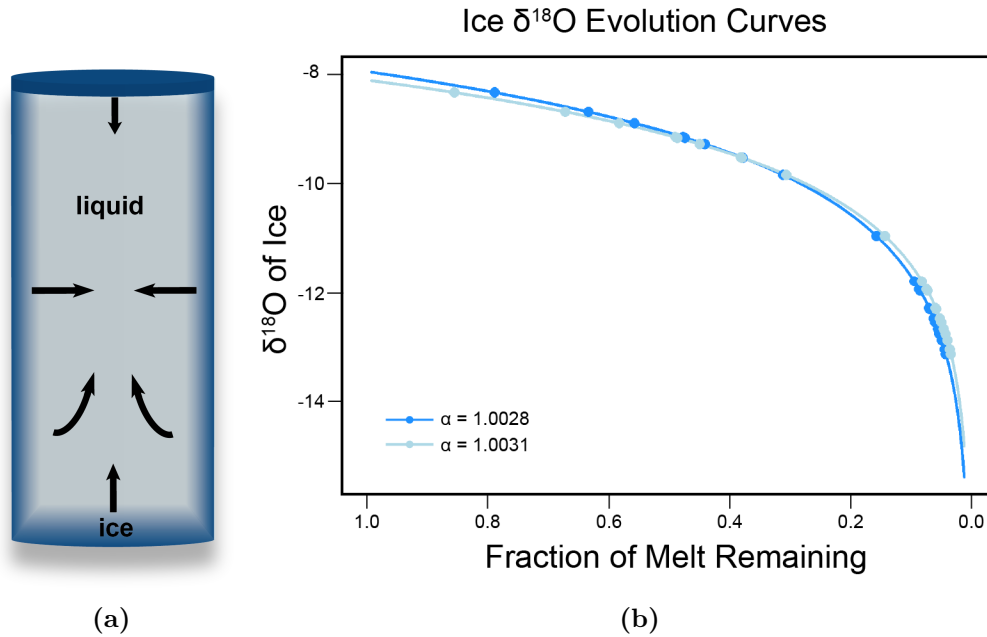


Figure 2: Exaggerated freezing pattern schematic (a) and the modeled evolution of $\delta^{18}\text{O}$ in ice column 2-A (b). Figure 2b employs a freezing boundary layer of 0.015 cm, freezing rate of 1.7 cm hr^{-1} and a diffusivity of ^{18}O in liquid water of $1.1 \times 10^{-5} \text{ cm}^2 \text{ sec}^{-1}$ following Lacelle et al. 2011. We believe the boundary layer to have been minimal at the onset of freezing due to vigorous mixing by the stir bar. Because the stir bar was immobilized during freezing, however, neither the boundary layer thickness nor the freezing rate were likely constant through time. Two different alpha values are used, 1.0031 and 1.0028, which correspond to the respective evolution curves. Samples from ice column 2-A are plotted along the curves.

2.2 Sublimation Experiments

We conducted two separate sublimation experiments utilizing two unique sets of methods. The first experiment was intended to maximize sublimation as its effects on sub-surface ice were not well-understood and no laboratory-based experiments known have attempted to evaluate this alteration below the immediate ice surface. The first experiment was therefore largely a sensitivity analysis to determine the responsiveness of the stable water isotope signal in sub-surface ice to short-term sublimation-maximized conditions. The second experiment more closely mimicked

the conditions of ground and shallow buried glacier ice in the McMurdo Dry Valleys region of Antarctica, a region where sublimation is known to be an important ablative process for glacier ice (Lamp and Marchant, 2017).

2.2.1 Sublimation-maximized experiment

Two columns of ice were frozen via the freezing methods described above. Immediately post-freezing, the cylinders were massed and a $\sim 9 \text{ cm}^2$ area of the exposed surface ice was chipped off and sampled. The cylinder caps used during freezing were then replaced with caps fitted with tubing for attachment to vacuum pumps. Following the emplacement of the custom cylinder caps, each cylinder was attached to a Fisher Air Cadet vacuum pump. The vacuum pumps served two purposes: (1) to evacuate the vapor out of the air gap in the cylinder, and (2) to reduce the pressure and thereby increase the melting temperature of ice and maximize sublimation, a practice commonly used in the freeze-drying of food (Franks, 1998). Manufacturer-reported maximum pressure for this pump model is 1.24 bars. The cylinders and the pumps were placed in the environmental chamber, set to maintain a temperature of $-2.0 \text{ }^\circ\text{C}$ and 20 % relative humidity.

The experiment ran for 498 hours (~ 20 days). The ambient chamber relative humidity remained within $\pm 3 \%$ of 19 %, and the chamber temperature remained within $\pm 0.1 \text{ }^\circ\text{C}$ of $-2.0 \text{ }^\circ\text{C}$. Following a brief power failure, the cylinders were removed from the chamber and placed in an auxiliary freezer for sampling. As the chamber is well-insulated, no liquid melt on the surface of the ice was observed as a result of the slightly increased temperatures due to the power failure.

Following the sampling method developed in the freezing experiments, the columns were subsequently halved using a table saw and the “inner cores” of each column were sampled. For each column, one half was sampled to depth at $\sim 2 \text{ cm}$ increments while the other was randomly sampled for quality control and an assessment of analytic uncertainty. Again, ice samples were removed using the hole saw, placed in clean

Ziploc bags with air extracted, and set to melt under room temperature conditions. Forty-four samples were collected from both ice columns combined in addition to the pre-sublimation surface ice samples. Immediately following the cessation of melting, the liquid was transferred via pipette into 5 ml glass sample vials for shipment to the Iowa State Department of Geological and Atmospheric Sciences Stable Isotope Lab where they were measured for δD and $\delta^{18}\text{O}$ using the methods described above. Summary data are reported for this experiment in Table 1 and all data are included in Appendix A.

2.2.2 Surface till sublimation experiment

The second sublimation experiment was intended to more-closely mimic, though not replicate, ground ice conditions in Mullins Valley, Antarctica and included simulated debris cover. Following the first sublimation experiment and the observed enrichment in the stable water isotope signals due to sublimation, we altered our methods slightly to increase experimental efficiency. We down-scaled the size of the cylinders to PVC tubes 4 inches (10.16 cm) in diameter which allowed us to sublimate more ice columns concurrently in the chamber. Additionally, as the magnitude of sublimation alteration was considerably greater than the noise due to freezing for the sublimation-maximized experiment, we dispensed with the cumbersome freezing methods described above in favor of less intensive procedures, detailed below.

The twelve PVC tubes 4 in. (10.16 cm) in diameter and 14 in. (35.56 cm) tall were therefore filled with 2.75 liters of well-mixed Poland Spring filtered water and placed in the environmental chamber set at +10.0 °C. The chamber then engaged in step-cooling, decreasing -1 °C every 3 minutes to -50 °C where it remained overnight (10 hours) until the liquid was completely frozen. Unlike in the first experiment, the cylinders were not capped during freezing. The ice was brought to 0 °C, increasing +1 °C every 2 minutes. One cylinder was removed from the chamber, cut into <2 cm width rings with a table saw, melted, and sent for ^{18}O and D measurement. The

remaining ice columns were used for the sublimation experiment.

As glacier and ground ice in the McMurdo Dry Valleys is commonly overlain by debris (Marchant and Head, 2007), we sought to replicate the debris cover using glass beads of known bulk density (2.6 g cm^{-3}) and diameter (150 - 210 μm). Rather than use previously-collected sediment and debris from the Dry Valleys, synthetic beads were used to more easily facilitate modeling of vapor diffusion through the till, following the methods of Lamp and Marchant (2017). This allowed for the calculation of an experimentally-derived relationship between debris depth and sublimation rate. Five debris depths were employed, with each depth applied to two of the eleven remaining ice columns. Additionally, 200 g of NaCl was added to one column of each debris depth, as it and other salts are commonly present in Dry Valleys debris cover. Table 2 reports the cylinder number, depth of debris, presence or absence of salt, total mass loss during sublimation (as a percent of initial mass), and the post-sublimation surface δD .

After freezing, the individual debris cover/salt mixtures were poured into ten of the cylinders. The cylinders were then massed, inclusive of the debris, prior to sublimation. HOBO environmental sensors were affixed to the rim of five of the cylinders to record conditions within the individual columns (see Fig. 1). Unlike in the sublimation maximized experiment, the cylinders were left uncovered during sublimation and the ambient chamber air was allowed to interact with the surface of the ice/debris. The ice was not sampled prior to sublimation so as to not alter the flat surface topography necessary for vapor diffusion modeling. Conditions within the environmental chamber remained within $\pm 0.2 \text{ }^\circ\text{C}$ of $-10.0 \text{ }^\circ\text{C}$ and $\pm 2\%$ of 20% RH. After sitting in the chamber for 475 hours (~ 19 days), the cylinders were removed and immediately massed. Seven of the ice columns were randomly selected for stable isotope analysis and sampled using the hole saw methods described above. The individual samples were melted in small Whirl-pack bags at room temperature and transferred via pipette to 5 ml glass scintillation vials for $\delta^{18}\text{O}$ and δD measurement at the Iowa State University

Department of Geological and Atmospheric Science Stable Isotope Lab. The analytical methods employed were the same as those used for previous samples, described above. Summary data for this experiment are reported in Table 2 and all data are included in Appendix A.

Experiments and Ice Column Names		
Experiment Name	Column Name	Sublimated (Y/N)
Freezing Methods Development	2-1	N
–	2-2	N
Sublimation-Maximized Experiment	3-1	Y
–	3-2	Y
Surface Till Experiment	4-3	Y
–	4-4	Y
–	4-9 ³	Y
–	4-10	Y
–	4-11	Y
–	4-12	Y

Table 1: Summary of core names for each experiment.

3 EXPERIMENTAL RESULTS

The data are divided by experiment and summary statistics for all sublimated ice columns are reported in Tables 1 and 2. See Appendix A for a list of all stable isotope values and other relevant data. Letters in ice column names correspond to that half of the column (cut lengthwise) which was sampled. Throughout this manuscript, cool colors in data figures indicate samples from ice columns that were not subjected to sublimation, whereas warm colors indicate samples from columns that underwent sublimation. The depths listed are the midpoint depth of the hole saw sampler.

Figure 3 reports final δ -values for the non-sublimated columns developed to serve as initial conditions to measure sublimation against. While both columns have near-homogeneous edge profiles, the centers of the columns are depleted relative to the edges and both become more enriched with depth—a function of the columns’ freezing

³Not included in analysis; see below.

pattern. Therefore, we were unsuccessful in developing a homogeneous ice column, as noted above. The data from these standard columns were included in Fig. 5, a composite plot of all $\delta^{18}\text{O}$ against δD for both sublimated and non-sublimated columns, from which the freezing water line and sublimation water line are calculated.

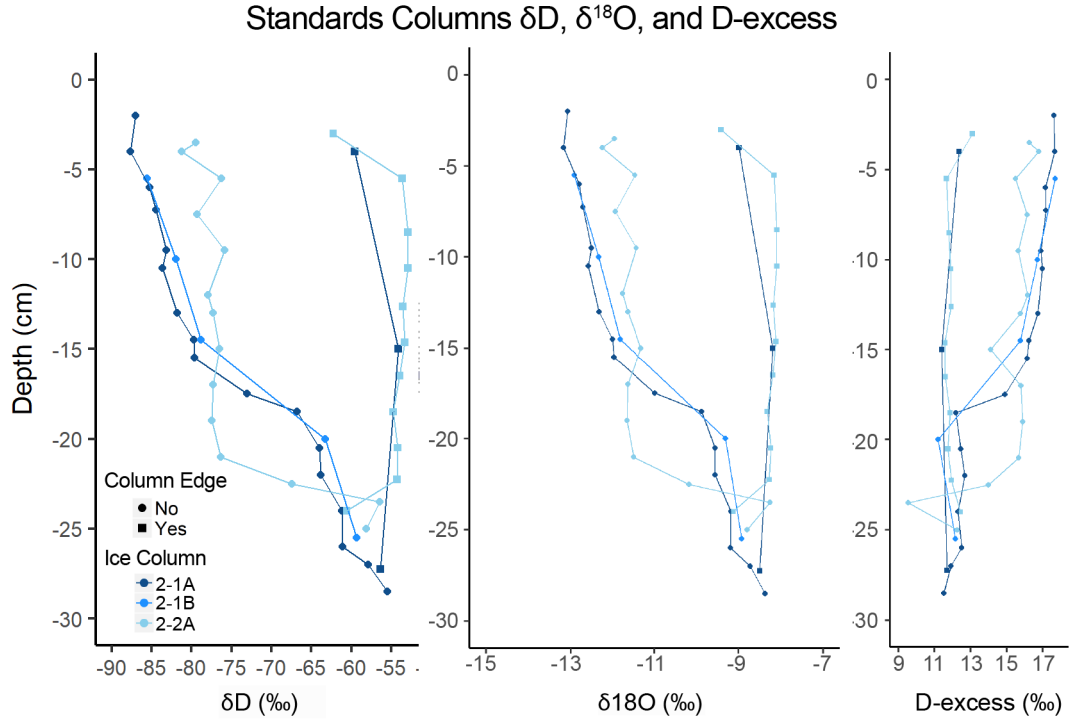


Figure 3: Depth profiles of δD , $\delta^{18}\text{O}$, and D-excess for the non-sublimated ice columns.

All columns experienced measurable net mass loss during sublimation, reported as a percent of initial mass in Tables 1 and 2. The stable isotope and D-excess profiles for the sublimated columns area shown in Fig. 4. They are characterized by both enrichment in the heavy isotope species and a corresponding decrease in d in the surface ice. While there were large differences in percent mass lost, we note no obvious differences in the magnitude of δ -alteration corresponding to amount of debris and/or the presence of salt in the debris mixture.

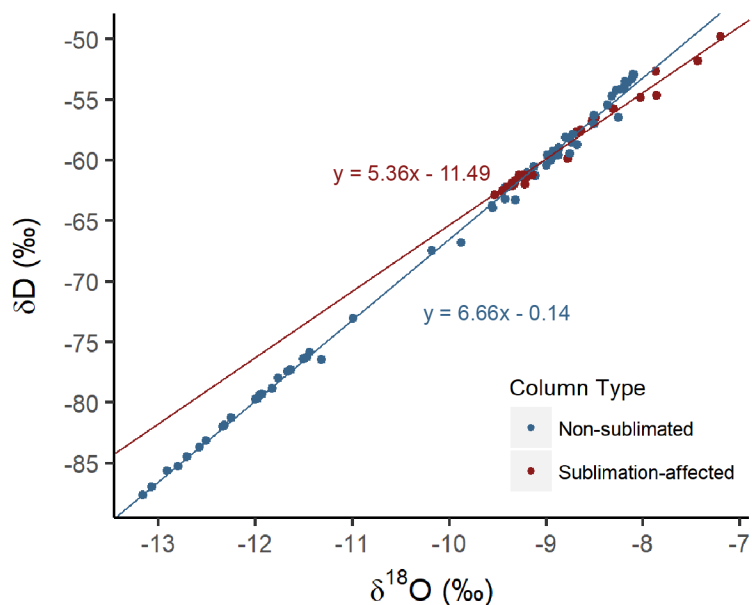


Figure 5: Plots of δD against $\delta^{18}O$ for all samples. The regression lines plotted are analogous to meteoric water lines (MWL). Here they are termed the “freezing water line” (FWL) and “sublimation water line” (SWL); see section 4.1 Evidence for sublimation-induced fractionation.

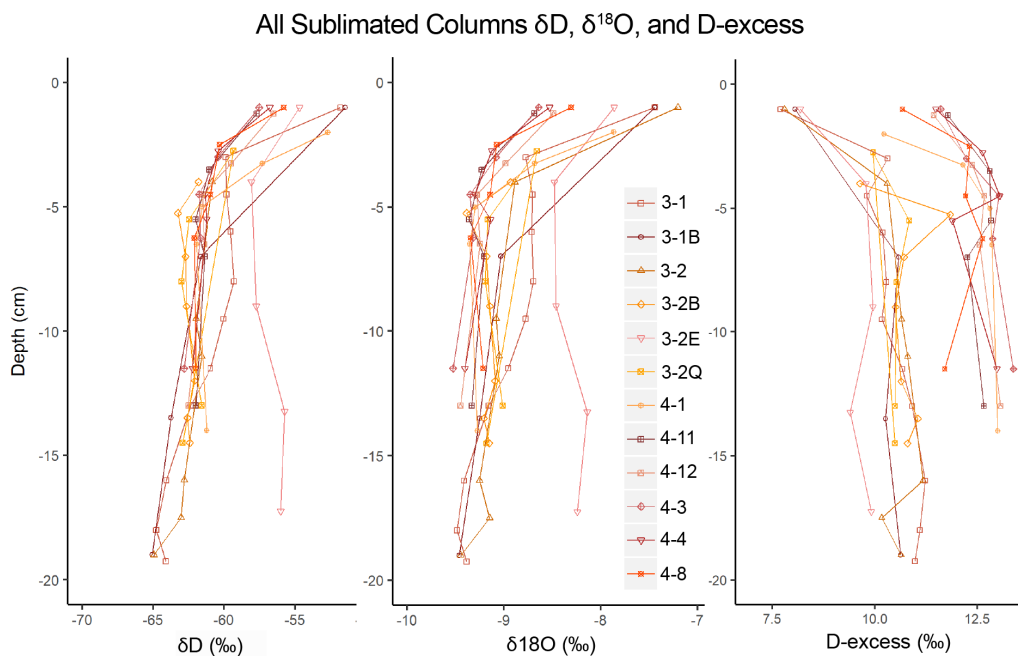


Figure 4: Depth profiles of δD , $\delta^{18}O$, and D-excess for the sublimated ice columns. Of note are the surface trends which suggest enrichment of the heavy isotope and a decrease in D-excess.

Break point analysis offers a statistical measure for identifying significant changes in the trend of the δ - and d -values at depth. This method uses an iterative approach to fit segmented-relationship regression models to our depth profile data (Muggeo, 2003). The 'segmented' R package can test for the presence or absence of break points and then subsequently estimate the break point value and its significance (Muggeo, 2008). Break point analyses were carried out for column 3-2, columns 3-1 and 3-2 combined, the combined surface sediment columns, and all sublimated columns combined. The break points for the composite all sublimated columns data set are reported as -3.62 cm for δD , -3.48 cm for $\delta^{18}O$ and -3.19 cm for d (Table 4).

One data point (03B-06) from column 03B was removed from the data set during analysis due to an errant d value of 14.83, which was considerably lower than any other value in the data set. We believe this discrepancy to be the result of instrumental error in the reporting of the sample's δD value, which was also very low. Statistical outlier analysis justified the omission of the sample. Data from column 4-9 were also omitted due to errors during sampling.

Summary Data for Sublimation-maximized Experiment				
Ice Column	Mass Loss (%)	Pre-Sublimation Surface δD ‰	Post-Sublimation Surface δD ‰	Sub-surface Mean δD ⁴
3-1	2.89	-60.31	-51.81	-61.95
3-2	2.99	-60.45	-49.80	-62.58

Table 2: Summary data for Experiment 1, the initial sublimation experiment designed to maximize ice sublimation. Columns were left to sublimate at -2 °C and 20 % relative humidity for 20 days.

⁴Mean values are calculated from post-sublimation samples and therefore do not include surface sample values.

Summary Data for Surface Debris Experiment				
Ice Column	Till Depth (cm)	Mass Loss (%)	Post-Sublimation Surface δD ‰	Salt (Y/N)
4-3	0.50	1.30	-57.52	Y
4-4	0.25	1.70	-56.75	Y
4-8	0.25	1.63	-55.77	N
4-9 ⁵	0.00	10.45	NA	N
4-10	2.00	0.23	-52.69	N
4-11	1.50	0.25	-57.69	N
4-12	0.50	0.66	-56.48	N

Table 3: Summary data for Experiment 2, the sublimation experiment with a mimicked surface “debris” of glass beads. Columns were left to sublimate at -10 °C and 20 % relative humidity for 19 days. Column 4-9 was omitted from analysis due to errors during sampling.

Break Points Summary Data			
Column(s)	δD Break Point (cm)	$\delta^{18}O$ Break Point (cm)	D-excess (d) Break Point (cm)
3-2	-3.262	-3.274	-4.885
3-1 & 3-2 Combined	-3.106	-3.072	-2.941
Combined Surface Debris Columns	-4.651	-4.396	-3.590
All Sublimated Columns	-3.621	-3.481	-3.190

Table 4: Break point depths for sublimated ice columns. Break points were calculated using the R statistical software ‘segmented’ package (Muggeo, 2008).

4 DISCUSSION

4.1 Evidence for sublimation-induced fractionation

4.1.1 Pre-sublimation and post-sublimation surface δD values

Visual analysis of Fig. 4 suggests two distinct paradigms: (1) an otherwise constant depth profile capped by (2) an enriched surface layer. Break point analysis (Table 4) confirms the significance of these two distinct trends. All statistical tests yielded p-values less than 0.05, suggesting that we can reject the null hypothesis that the difference between the linear regression slope of the surface ice and the ice at depth is 0; in other words, the two slopes are statistically not equal. That the break point

⁵Not included in analysis due to errors during sampling.

depths estimated for both δD and $\delta^{18}O$ are similar for all data sets is not surprising, as the two values are linked via the physics governing fractionation. The break points identified for d differ from those calculated for δD and $\delta^{18}O$, with the largest deviation in ice column 3, for which the d break point is estimated to be almost 1.5 cm deeper than those for the δ -values. We believe the discrepancies in predicted depth to be of secondary importance as the low sampling resolution and sample N both prohibit robust determination of an effect depth. That said, these depths are in agreement with other field based studies that suggest an effect from sublimation in buried glacier ice below the immediate ice surface (Lacelle et al., 2011).

Having established that our samples collected nearer the ice surface have been subjected to alteration, we can identify that process which has occurred using metrics common in isotope hydrology. In experiment 2, the “sublimation-maximized” experiment, surface samples collected prior to sublimation were considerably more depleted compared to those collected following sublimation (Table 2). Because mass loss at the surface induces a downward migration of the ice-air interface through the original core, samples collected at the surface following the experiment were not expected to be identical, even in un-altered ice. The approximate surface height change for the sublimation-maximized columns 2 and 3 (calculated from total volume lost using an ice density of 0.9167 g cm^{-3})⁶ were 1.5 cm and 1.17 cm, respectively. The surface δD values following sublimation were notably enriched, increasing +8.5 ‰ in column 2 and +10.65 ‰ in column 3. Prior to sublimation, surface δD values registered very near to the sub-surface δD mean (Table 2) and slightly more depleted than the shallow subsurface (<5 cm depth) samples, whereas following sublimation they were significantly more enriched than both of those metrics. Post-sublimation surface values for both columns 2 and 3 were more than 3.5 standard deviations away from the sub-surface mean. As such, the difference cannot be explained simply as the result of removing the top ~1.5 cm of ice and instead suggests alteration in surface ice in

⁶This calculation assumes no change in porosity, which is unlikely.

agreement with Sokratov and Golubev (2009) who observed enrichment in shallow surface ice (<4 mm) following their controlled sublimation experiments.

4.1.2 Comparison of the meteoric, freezing and sublimation water line slopes

Comparison of the “water lines” for sublimated and unsublimated ice provide further evidence for an alternative sublimation effect. As noted in the Theoretical Background above, the slope of the regression line of $\delta^{18}\text{O}$ and δD (lines analogous to the MWL) is correlated with changes in phase (Souchez and Jouzel, 1984; Lacelle, 2011; Clark and Fritz, 1997; Kim and Lee, 2011). Determination of the slope of the “freezing water line” (FWL) by Souchez and Merlivat (1984) yielded differing values corresponding to unique water sources. The slope of the FWL for Antarctic water was 4.37, for Arctic water 5.99, and for alpine water the FWL slope was 6.63. O’Neil (1968) and Suzuoka (1973) determined the FWL slope to be 6.18 and 7.19, respectively, for their equilibrium-freezing experiments. The slope of the WL for liquid reservoirs having undergone evaporation are additionally much lower than the MWL and FWL, between 2 and 5 (Clark and Fritz, 1997; Kim and Lee, 2011). We divided our samples into two subsets: those having been altered by sublimation and those presumed to be relatively unaltered. Employing a conservative estimate of the sublimation effect depth, only the uppermost samples of each sublimated core were included as “sublimation-affected” samples, and “non-sublimated” samples were those from cores either having not undergone sublimation (the “Standards Columns”) or from depths lower than -5 cm in the sublimated cores. All other values were not included in the analysis.

The slope of our FWL ($S = 6.65$, $R^2 = 0.998$) shows excellent agreement with the previous experimentally-derived FWL slopes, particularly that of Souchez and Jouzel’s (1984) ($S = 6.63$). Further, the slope of our SWL ($S = 5.36$, $R^2 = 0.934$) is lower than the FWL and closer to that for evaporation, within the bounds expected for sublimation. This is indicative of sublimation (Sokratov and Golubev, 2009; Lacelle et al., 2011), and is very near the surface ice slope ($S = 5.1$) of Lacelle et al.

(2011)—calculated from samples of relict ice that was known to have experienced prolonged sublimation.

4.1.3 Mass balance of the post-sublimation columns

For a fourth and final check on our data, we used a mass balance approach to calculate an initial, pre-freezing bulk water δD which could then be compared with the measured bulk water value using Equation 5:

$$\delta D_{bulk} = f_{ice} * \delta D_{ice} + f_{vapor} * \delta D_{vapor} \quad (5)$$

where f is equal to the volume fraction of the water in each phase following the experiment, such that

$$f_{ice} + f_{vapor} = 1, \quad (6)$$

and

$$f_{ice} = \frac{\text{Vol}_{(Post)} (\text{cm}^3)}{\text{Vol}_{(Pre)} (\text{cm}^3)}. \quad (7)$$

As we did not capture the vapor generated from our sublimating ice columns, we were unable to utilize a measured δD_{vapor} . To proceed with our mass balance calculations we instead approximated a theoretical δD_{vapor} using α -values for sublimation fractionation at -10 °C and the δD value of the surface ice prior to sublimation, following Equations 8 and 9:

$$\alpha_{solid-vapor} = \frac{\left(\frac{D}{H}\right)_{ice}}{\left(\frac{D}{H}\right)_{vapor}}, \quad (8)$$

where

$$\left(\frac{D}{H}\right)_{VSMOW} = 0.015574 \text{ (Baertschi, 1976)}. \quad (9)$$

The δD of the ice is neither constant throughout nor equally represented among our samples, therefore a simple average of all the column data would incorrectly weight the total ice δD with the depleted “inner core” values. We computed a weighted average to more accurately approximate the δD of the entire frozen column. The ice column was therefore subdivided into two volumes: (1) a depleted center core and (2) the enriched outer edge. A diameter of 7 cm was employed to calculate the volume of the inner core as this is the approximate width of the sampling profile. Using a smaller radius would include more of the enriched outer core, ignoring the gradient in δD values from the edge of the column to the center and thus overestimating the net enrichment due to sublimation. Therefore, we believe 7 cm allows for a conservative approximation of the weighted average.

Mass Balance Calculations				
Study	Temperature (°C)	α	Calculated Vapor δD (‰)	Calculated Bulk Water δD (‰)
Ellehoj et al. (2017)	-10.15	1.164	-192.83	-61.59
–	-10.05	1.157	-187.94	-61.45
–	-9.95	1.163	-192.13	-61.57
–	-9.95	1.157	-187.94	-61.45
Merlivat and Nief (1967)	-10.7	1.150	-183.00	-61.30
–	-10.6	1.153	-185.13	-61.36
–	-10.5	1.153	-185.13	-61.36
–	-10.4	1.152	-184.4	-61.34

Table 5: Vapor and bulk liquid δD calculated using fractionation factors (α) reported in the experimental literature. The measured bulk water value is -56.6 ‰. Due to the variability in the reported α -values, we observe a 10‰ range in our calculated vapor δD . This variability is not present in the calculated bulk water values because much less material sublimated off compared to the amount that remained in the solid phase.

As mentioned in the Theoretical Background above, we employ a range of fractionation factors (α) for the mass balance calculations due to variability in the literature-

reported values. The theoretical δD of our vapor calculated using the pre-sublimation surface ice δD ranges from -192.13 ‰ to -183.00 ‰ (Table 5). The calculated initial bulk water δD for column 3 ranges from -61.59 ‰ to -61.30 ‰ whereas the (averaged) measured value for column 3 water pre-freezing was -56.60 ‰ (Table 5). Our calculation assumes equally-spaced δD samples and does not consider sublimation following freezing but before measurement of the pre-sublimation mass and surface δD . It is thus not an effort to perfectly replicate the initial bulk water value, but rather to demonstrate that the amount of material lost due to sublimation could reasonably explain the enrichment we observe at the surface. As our calculated initial value is more depleted than the measured, it appears to under- rather than over-estimate the effect of sublimation. The depleted values in the shallow ice sub-surface are washed out in the bulk average, which could additionally contribute to the under-estimation of the net sublimation effect. We take this approximation, in addition to (1) our pre/post surface ice measurements; (2) comparison of the SWL and FWL slopes; and (3) the significant breaks in the trend of δD with depth as convincing evidence that sublimation-induced fractionation has altered the stable isotope values at the surface of our ice columns and very possibly the ice at greater depths.

4.2 Proposed mechanism for alteration at depth

The molecular diffusivity of solid ice is extremely low (appx. $1.49 \times 10^{-11} \text{ cm}^2 \text{ sec}^{-1}$) (Ramseier, 1967), and therefore alteration of the stable isotope signal at depth via solid-state diffusion within the ice grains is not expected on laboratory time scales. This said, diffusivity at grain boundaries in polycrystalline ice is over three orders of magnitude higher than that for diffusion in the water ice lattice ($3.0 \times 10^{-7} \text{ cm}^2 \text{ sec}^{-1}$) (Nasello et al., 2007), providing a mechanism for diffusion at depth within the ice. Investigations of diffusion in ice cores suggests that the presence of liquid films at polycrystalline ice grain boundaries, themselves commonly formed due to impurities, can enhance diffusion within solid ice (Johnsen et al., 2000; Nye, 1998),

thereby displacing the climate signal (Rempel et al., 2001). As our ice is certainly polycrystalline (rapid freezing time and non-unidirectional freezing), it is reasonable to infer that diffusion occurs along grain boundaries within our manufactured ice columns. We apply this idea, initially proposed by Lacelle et al. (2011) as the mechanism for diffusion following sublimation in ice from University Valley, Antarctica, to explain the propagation of the sublimation signal to sub-surface depths.

Sublimation occurs in our experiment primarily due to the pronounced gradient in the partial pressure of water vapor within the chamber. As the chamber evacuates the air to maintain low RH, the column of ice (presumably at 100% RH) sublimates to compensate for this deficit. This sublimation then drives a preferential fractionation of the light isotopes into the vapor phase, enriching the remaining surface ice in the heavy isotope. The increase in the abundance of heavy isotope at the surface therefore induces downward Fickian diffusion in the remaining ice along grain boundaries (Lacelle et al., 2011), and a dynamic equilibrium is maintained so long as the surface continues to sublimate. A forthcoming modeling study, Ehrenfeucht and Dennis (2018, in preparation), describes this mechanism in greater detail. Figure 6 provides a simplified illustration.

4.3 Implications for paleoclimate reconstructions using surface-exposed ice

Glacier ice has long been understood to be an excellent record of paleoclimate, and considerable effort has been devoted to the recovery and analysis of ice cores from polar and high-alpine areas. Most ice cores, regardless of the glacial environment, are drilled at ice divides in the accumulation zone to avoid post-deposition complications from the flow of ice (Lorius et al., 1979; Morgan et al., 1997; Dansgaard et al., 1982). As discussed above, the effects of diffusion and sublimation within snow and firn have been well-studied [e.g. Ebner et al. (2017), Neumann et al. (2008), Van Der Wel et al. (2011), and Stichler et al. (2001)], and this investigation has limited applications for studies on ice cores from regions where the snow-firn-glacier ice gradient is substantially

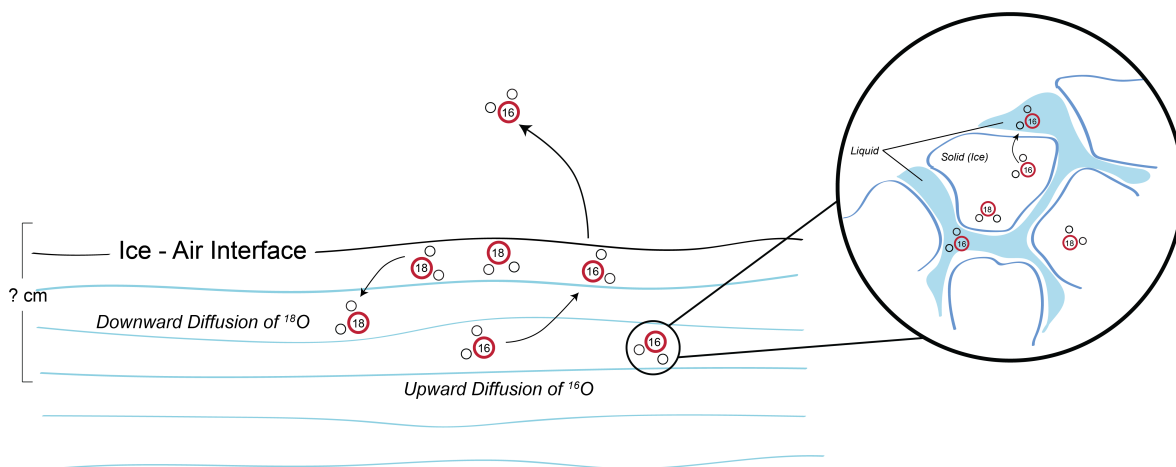


Figure 6: Theoretical schematic illustrating the effect of sublimation on isotope abundances at the ice surface. As the surface is enriched in the heavy isotopologues, the heavier molecules diffuse downwards away from the sublimation front. Thin liquid films described by Nye et al. [1998] facilitate the diffusion of these heavier isotopologues more quickly than would be anticipated via solid-state diffusion.

thick. This experimental work is thus most-appropriately applied to paleoclimate reconstructions derived from areas of ice exposed to the atmosphere, particularly those in Antarctica, where sublimation is common.

Over the past several decades, increased attention has been devoted to the “blue ice” areas of East Antarctica where patches of ancient ice believed to be older than 1 Ma have been exposed at the surface due to unique glaciological conditions (Spaulding et al., 2013; Fogwill et al., 2017; Machida et al., 1996; Winter et al., 2016; Higgins et al., 2015). Many of these studies utilize stable water isotope ratios of ice collected at, or very near, the surface (between 5 cm and 20 cm depth) as proxies for paleothermometric reconstructions. Given that our results suggest sublimation likely alters the stable isotopes ratios of surface and potentially shallow sub-surface ice, we recommend caution when utilizing exposed ice for paleoclimate interpretations. Spaulding et al. (2013) assess the potential for sublimation-induced alteration of surface ice by comparing their samples’ δ -values with others from well-dated ice core horizons, including an ash layer. Interestingly, after correction for differences in the time/depth scale and resolution, they note strong correlation between their surface values and those from

the ice cores at depth, indicating minimal alteration due to sublimation (Spaulding et al., 2013). Therefore, it appears as though surface-exposed ice may still contain important climate records, though our study results suggest that careful investigation of potential alteration at and below the surface is necessary prior to the extrapolation of a paleoclimate record. As each study site is subjected to unique environmental conditions that affect the sublimation rate, isotope composition of the corresponding vapor, and potential diffusion at depth, determination of the sublimation-induced alteration potential is necessary at each site and cannot be ruled out *a priori*.

4.4 Study limitations and future directions

This study has several limitations as mentioned above but delineated in clear detail here. First and foremost, we are limited by relatively low-resolution data (~ 2 cm) despite studying an alteration that occurs at rather small scales. This subverts our ability to describe, through experimental observations, the nature of diffusion in the ice sub-surface, the magnitude of alteration at depth, and the maximum depth of alteration. However, the employed ~ 2 cm sample diameter was the minimum allowable size to retrieve a sufficient volume of non-edge, inner-core ice for repeat measurements in the Picarro spectrometer. As such, future studies would benefit from much lower resolution, perhaps by shaving mm-thick layers of ice as in Sokratov and Golubev (2009).

Though not necessarily a limitation of our study, future investigations of the ice would benefit greatly from continuous vapor measurements collected during the experimental run, such as those performed by Brown et al. (2012) and Ellehoj et al. (2013). These measurements would facilitate precise comparison between the evolution of the vapor and the post-sublimation stable isotope signal of the ice. This could be achieved by replacing the vacuum pump tubes in our “sublimation-maximized” experiment with those attached to a spectrometer vapor analysis system, such as those developed and sold by Picarro. We did not have access to such an instrument and

therefore were unable to make these measurements.

Additionally, we note the obvious challenge of assessing the magnitude of alteration at depth without clear measurements of the pre-sublimation values below the surface, given the variations in freezing patterns. We chose not to halve the cores prior to sublimation in order to avoid possible edge effects at the interface between the flat “inner column” face and the PVC edge. Additionally, cylindrical containers allowed for more straightforward model development as compared to half-cylindrical. Having completed these whole-column sublimation experiments, however, we are currently engaging in a series of experiments which will allow for a more robust pre/post assessment of sublimation alteration below the ice surface. The ice columns in these new experiments are halved post-freezing, and one half of each column is immediately sampled to depth. The other half of each column is then placed in a specially-machined half-cylinder sublimation container. This series of experiments will likely assist in constraining the magnitude of diffusion/alteration at depth.

Finally, the many differences between glacial ice formed by snow compression and ice manufactured in the lab cannot be ignored. In particular, structural differences in the ice matrix could have important implications for the suggested diffusion at ice grain boundaries. Grain size is of particular importance, as increased surface area and smaller ice grain volumes could lead to enhanced diffusion. It has previously been established that the sublimation rate and vapor isotope composition can depend strongly on the density of the surface ice, which is known to evolve over the course of sublimation and can vary depending on crystal grain size (Brown et al., 2012). Therefore, a robust assessment of ice crystallographic changes resulting from sublimation would be useful for understanding the alteration occurring at the surface, which may differ depending on the unique, in-situ ice conditions (e.g. micro-fracturing, bubble density, etc.).

In addressing these limitations to our study, we suggest further investigation of the effects of sublimation on glacier ice, building on the preliminary experimental data reported herein. This is particularly important for paleoclimate studies based on

atmosphere-exposed ice. We cite our ability to affect a change in the stable isotope ratios of our ice columns over short, laboratory timescales as evidence that the influence of sublimation on isotope abundances cannot be ignored *a priori* for ice exposed to the atmosphere. We believe this work provides a useful first-order assessment of these sublimation-induced effects, despite the aforementioned study limitations.

5 CONCLUSIONS

We present the results of our study investigating the effect of sublimation on the stable isotope ratios of surface, sub-surface, and buried ice. Our data suggests that sublimation has a measurable effect on stable isotope ratios, contrary to the assumption that “layer-by-layer” sublimation prohibits the alteration of in-situ ice (Dansgaard, 1964; Dansgaard et al., 1973; Friedman et al., 1991). This has been determined through (1) analysis of pre- and post-sublimation surface ice δ -values; (2) comparison of our ice’s SWL and FWL slopes to those in the existing literature; (3) the statistical determination of two distinct slopes in the profiles of ice δ -values at depth; (4) isotope mass balance reconstructions. We additionally note a potential effect from sublimation not only in samples within 2 cm of the surface, but also in samples in the shallow sub-surface at less than ~ 4 cm depth.

As such, our investigation agrees with other previous experimental and field studies that observe fractionation due to sublimation (Sokratov and Golubev, 2009; Lécuyer et al., 2017; Brown et al., 2012; Grootes et al., 1989). It shows striking similarity to data from Lacelle et al. (2011), one of the few studies to investigate the effect of sublimation on ice collected in the field. Furthermore, we agree with the mechanism employed by Lacelle et al. (2011) and discussed in Brown et al. (2012), which suggests that diffusion at grain edge boundaries may enhance diffusion within solid ice, as suggested by Rempel et al. (2001). This may have important implications for studies using the stable isotope ratios of ice exposed at the surface for paleoclimate reconstructions [e.g. Sinisalo et al. (2007), Moore et al. (2006), Turney et al. (2013), and Spaulding et al. (2013)], as both the surface and sub-surface ice are subject to potential alteration. Unlike laboratory experiments, however, field ice is subjected to innumerable possible conditions that may affect sublimation. Therefore we recommend thorough investigation of the effects of sublimation prior to the extrapolation of a climate record, as these effects may have important implications for the corresponding paleoclimate interpretations.

A APPENDIX: ALL DATA

All Data							
Sample	Edge	Core	Mass Change	Depth	$\delta^{18}\text{O}$	δD	d
02-01	N	2	251.92	-1	-7.44	-51.81	7.7
02-02	N	2	251.92	-3	-8.77	-59.89	10.31
02-03	N	2	251.92	-4.5	-8.7	-59.81	9.81
02-04	N	2	251.92	-6	-8.71	-59.52	10.19
02-05	N	2	251.92	-8	-8.7	-59.3	10.28
02-06	N	2	251.92	-9.5	-8.77	-60.02	10.17
02-07	N	2	251.92	-11.5	-8.95	-60.97	10.67
02-08	N	2	251.92	-13	-9.16	-62.37	10.91
02-09	N	2	251.92	-16	-9.41	-64.07	11.23
02-10	N	2	251.92	-18	-9.48	-64.78	11.09
02-11	N	2	251.92	-19.25	-9.39	-64.11	10.98
02B-1	N	2B	251.92	-1	-7.44	-51.46	8.06
02B-2	N	2B	251.92	-7	-9.03	-61.66	10.56
02B-3	N	2B	251.92	-13.5	-9.25	-63.74	10.27
02B-4	N	2B	251.92	-19	-9.46	-65.05	10.61
02P-T1	N	2	NA	0	-8.75	-60.31	9.73
03P-T1	N	3	NA	0	-8.81	-60.45	10.02
02PE-T1	Y	2	NA	0	-9.75	-65.93	12.11
02PE-T2	Y	2	NA	0	-9.72	-65.84	11.92
BWPF-01	N	BULK	NA	0	-7.39	-55.34	3.81
BWPF-02	N	BULK	NA	0	-7.29	-54.57	3.76
02PF-01	N	BULK	NA	0	-8.21	-56.97	8.71
02PF-02	N	BULK	NA	0	-8.21	-56.8	8.85
03PF-01	N	BULK	NA	0	-7.77	-55.64	6.5
03PF-02	N	BULK	NA	0	-8.12	-57.57	7.39
03-05Q-02	N	3Q	195.68	-14.5	-9.18	-62.93	10.49
03E-01	Y	3E	195.68	-1	-7.86	-54.69	8.21
03E-02	Y	3E	195.68	-4	-8.48	-58.06	9.77
03E-03	Y	3E	195.68	-9	-8.46	-57.73	9.96
03E-04	Y	3E	195.68	-13.25	-8.14	-55.72	9.42
03E-05	Y	3E	195.68	-17.25	-8.24	-56.01	9.94
03-01	N	3	195.68	-1	-7.2	-49.8	7.84
03-02	N	3	195.68	-4	-8.89	-60.82	10.3
03-03	N	3	195.68	-9.5	-9.08	-62	10.64
03-04	N	3	195.68	-11	-9.05	-61.6	10.82
03-05	N	3	195.68	-16	-9.25	-62.82	11.17
03-06	N	3	195.68	-17.5	-9.15	-63.03	10.17
03-07	N	3	195.68	-19	-9.45	-64.96	10.67
03B-01	N	3B	195.68	-2	-8.02	-54.86	9.34

Sample	Edge	Core	Mass Change	Depth	$\delta^{18}\text{O}$	δD	d
03B-02	N	3B	195.68	-4	-8.93	-61.82	9.63
03B-03	N	3B	195.68	-5.25	-9.39	-63.27	11.84
03B-04	N	3B	195.68	-7	-9.18	-62.74	10.71
03B-05	N	3B	195.68	-9	-9.15	-62.67	10.5
03B-07	N	3B	195.68	-12	-9.09	-62.09	10.64
03B-08	N	3B	195.68	-13.5	-9.21	-62.6	11.05
03-01Q	N	3Q	195.68	-2.75	-8.66	-59.31	9.96
03-02Q	N	3Q	195.68	-5.5	-9.17	-62.48	10.84
03-03Q	N	3Q	195.68	-8	-9.19	-63.02	10.52
03-04Q	N	3Q	195.68	-13	-9.01	-61.61	10.49
03-05Q-01	N	3B	195.68	-14.5	-9.15	-62.44	10.79
GB03-01	N	4-3	43.73	-1	-8.64	-57.52	11.61
GB03-02	N	4-3	43.73	-3	-9.08	-60.42	12.23
GB03-03	N	4-3	43.73	-4.5	-9.35	-61.78	13.02
GB03-04	N	4-3	43.73	-6.25	-9.32	-61.68	12.87
GB03-05	N	4-3	43.73	-11.5	-9.53	-62.84	13.37
GB04-01	N	4-4	58.34	-1	-8.53	-56.76	11.48
GB04-02	N	4-4	58.34	-2.75	-9.13	-60.39	12.62
GB04-03	N	4-4	58.34	-4.5	-9.3	-61.35	13.05
GB04-04	N	4-4	58.34	-5.5	-9.14	-61.23	11.89
GB04-05	N	4-4	58.34	-11.5	-9.4	-62.25	12.97
GB08-01	N	4-8	55.76	-1	-8.31	-55.77	10.67
GB08-02	N	4-8	55.76	-2.5	-9.08	-60.31	12.31
GB08-03	N	4-8	55.76	-4.5	-9.14	-60.94	12.21
GB08-04	N	4-8	55.76	-6.25	-9.34	-62.13	12.62
GB08-05	N	4-8	55.76	-11.5	-9.21	-62.01	11.7
GB10-01	N	4-10	7.85	-2	-7.86	-52.69	10.22
GB10-02	N	4-10	7.85	-3.25	-8.68	-57.29	12.15
GB10-03	N	4-10	7.85	-5	-9.3	-61.56	12.81
GB10-04	N	4-10	7.85	-6.5	-9.35	-61.98	12.86
GB10-05	N	4-10	7.85	-14	-9.28	-61.21	12.99
GB11-01	N	4-11	8.35	-1.25	-8.68	-57.7	11.78
GB11-02	N	4-11	8.35	-3.5	-9.23	-61.04	12.8
GB11-03	N	4-11	8.35	-5.5	-9.36	-62.02	12.84
GB11-04	N	4-11	8.35	-7	-9.2	-61.38	12.26
GB11-05	N	4-11	8.35	-13	-9.33	-62.01	12.65
GB12-01	N	4-12	22.15	-1.25	-8.49	-56.48	11.44
GB12-02	N	4-12	22.15	-3.25	-8.98	-59.49	12.38
GB12-03	N	4-12	22.15	-4.5	-9.28	-61.55	12.67
GB12-04	N	4-12	22.15	-6.5	-9.25	-61.42	12.56
GB12-05	N	4-12	22.15	-13	-9.45	-62.53	13.07
JugA	NA	BULK	NA	0	-9	-60.27	11.69
JugB	NA	BULK	NA	0	-7.96	-57.65	6.02

Sample	Edge	Core	Mass Change	Depth	$\delta^{18}\text{O}$	δD	d
A1	N	2-A	NA	-2	-13.07	-86.97	17.62
A2	N	2-A	NA	-4	-13.16	-87.61	17.68
A3	N	2-A	NA	-6	-12.8	-85.23	17.15
A4	N	2-A	NA	-7.25	-12.71	-84.47	17.18
A5	N	2-A	NA	-9.5	-12.51	-83.15	16.92
A6	N	2-A	NA	-10.5	-12.58	-83.66	16.98
A7	N	2-A	NA	-13	-12.32	-81.82	16.73
A8	N	2-A	NA	-14.5	-12	-79.73	16.25
A9	N	2-A	NA	-15.5	-11.97	-79.65	16.15
A10	N	2-A	NA	-17.5	-10.99	-73.04	14.91
A11	N	2-A	NA	-18.5	-9.87	-66.8	12.2
A12	N	2-A	NA	-20.5	-9.55	-63.97	12.46
A13	N	2-A	NA	-22	-9.56	-63.79	12.69
A14	N	2-A	NA	-24	-9.19	-61.17	12.31
A15	N	2-A	NA	-26	-9.2	-61.06	12.51
A16	N	2-A	NA	-27	-8.72	-57.86	11.92
A17	N	2-A	NA	-28.5	-8.37	-55.44	11.52
A18	Y	2-A	NA	-4	-8.99	-59.57	12.36
A19	Y	2-A	NA	-15	-8.19	-54.12	11.41
A20	Y	2-A	NA	-27.25	-8.5	-56.33	11.69
A21	N	2-B	NA	-5.5	-12.91	-85.59	17.7
A22	N	2-B	NA	-10	-12.34	-81.98	16.71
A24	N	2-B	NA	-14.5	-11.82	-78.82	15.77
A25	N	2-B	NA	-20	-9.31	-63.3	11.2
A23	N	2-B	NA	-25.5	-8.93	-59.29	12.16
B1	N	3-A	NA	-3.5	-11.96	-79.44	16.26
B2	N	3-A	NA	-4	-12.25	-81.22	16.79
B3	N	3-A	NA	-5.5	-11.47	-76.27	15.49
B4	N	3-A	NA	-7.5	-11.93	-79.33	16.15
B5	N	3-A	NA	-9.5	-11.44	-75.86	15.65
B6	N	3-A	NA	-12	-11.76	-77.95	16.17
B7	N	3-A	NA	-13	-11.64	-77.33	15.78
B8	N	3-A	NA	-15	-11.32	-76.46	14.11
B9	N	3-A	NA	-17	-11.64	-77.32	15.8
B10	N	3-A	NA	-19	-11.67	-77.44	15.89
B11	N	3-A	NA	-21	-11.5	-76.37	15.67
B12	N	3-A	NA	-22.5	-10.18	-67.46	13.99
B13	N	3-A	NA	-23.5	-8.25	-56.47	9.56
B14	N	3-A	NA	-25	-8.8	-58.15	12.27
B15	Y	3-A	NA	-3	-9.42	-62.26	13.11
B16	Y	3-A	NA	-5.5	-8.16	-53.61	11.67

Sample	Edge	Core	Mass Change	Depth	$\delta^{18}\text{O}$	δD	d
B17	Y	3-A	NA	-8.5	-8.09	-52.94	11.81
B18	Y	3-A	NA	-10.5	-8.1	-52.9	11.89
B19	Y	3-A	NA	-12.625	-8.18	-53.54	11.93
B20	Y	3-A	NA	-14.625	-8.11	-53.33	11.58
B21	Y	3-A	NA	-16.5	-8.2	-53.97	11.6
B22	Y	3-A	NA	-18.5	-8.32	-54.73	11.86
B23	Y	3-A	NA	-20.5	-8.24	-54.18	11.74
B24	Y	3-A	NA	-22.25	-8.28	-54.27	11.95
B25	Y	3-A	NA	-24	-9.13	-60.57	12.45
C1	N	BULK	NA	0	-9.59	-64.98	11.78
C2	N	BULK	NA	0	-9.54	-63.84	12.47
C3	N	BULK	NA	0	-9.22	-61.38	12.34

References

- Baertschi, P. (1976). Absolute ^{18}O content of standard mean ocean water. *Earth and Planetary Science Letters*, 31(3):341–344.
- Brown, R. H., Lauretta, D. S., Schmidt, B., and Moores, J. (2012). Experimental and theoretical simulations of ice sublimation with implications for the chemical, isotopic, and physical evolution of icy objects. *Planetary and Space Science*, 60(1):166–180.
- Casado, M., Landais, A., Picard, G., Münch, T., Laepple, T., Stenni, B., Dreossi, G., Ekaykin, A., Arnaud, L., Genthon, C., Touzeau, A., Masson-Delmotte, V., and Jouzel, J. (2016). Archival of the water stable isotope signal in East Antarctic ice cores. *The Cryosphere*, (November):1–33.
- Clark, I. D. and Fritz, P. (1997). *Environmental Isotopes in Hydrogeology*. Lewis Publishers.
- Dansgaard, W. (1964). Stable isotopes in precipitation. *Tellus*, 16(4):436–468.
- Dansgaard, W., Clausen, H., Gundestrup, N., Hammer, C., Johnsen, S. J., Kristinsdottir, P., and Reeh, N. (1982). A New Greenland Deep Ice Core. *Science*, 218(4579):1273–1277.
- Dansgaard, W., Johnsen, S., Clausen, H. B., and Gundestrup, N. (1973). *Stable Isotope Glaciology*.
- Ebner, P. P., Steen-Larsen, H. C., Stenni, B., Schneebeli, M., and Steinfeld, A. (2017). Experimental observation of transient $\delta^{18}\text{O}$ interaction between snow and advective airflow. *The Cryosphere*, (11):1733–1743.
- Ekaykin, A. A., Hondoh, T., Lipenkov, V., and Miyamoto, A. (2009). Post-depositional changes in snow isotope content : preliminary results of laboratory experiments. *Climate of the Past Discussions*, 5(October):2239–2267.
- Ellehoj, M. D., Steen-Larsen, H. C., Johnsen, S. J., and Madsen, M. B. (2013). Ice-vapor equilibrium fractionation factor of hydrogen and oxygen isotopes: Experimental investigations and implications for stable water isotope studies. *Rapid Communications in Mass Spectrometry*, 27(19):2149–2158.
- EPICA Community Members (2004). Eight glacial cycles from an Antarctic ice core. *Nature*, 429:623–628.
- Fisher, D. A. and Lacelle, D. (2014). A model for co-isotopic signatures of evolving ground ice in the cold dry environments of Earth and Mars. *Icarus*, 243:454–470.
- Fogwill, C. J., Turney, C. S., Golledge, N. R., Etheridge, D. M., Rubino, M., Thornton, D. P., Baker, A., Woodward, J., Winter, K., Van Ommen, T. D., Moy, A. D., Curran, M. A., Davies, S. M., Weber, M. E., Bird, M. I., Munksgaard, N. C., Menviel, L., Rootes, C. M., Ellis, B., Millman, H., Vohra, J., Rivera, A., and Cooper, A. (2017).

- Antarctic ice sheet discharge driven by atmosphere-ocean feedbacks at the Last Glacial Termination. *Scientific Reports*, 7(October 2016):1–10.
- Franks, F. (1998). Freeze-drying of bioproducts: Putting principles into practice. *European Journal of Pharmaceutics and Biopharmaceutics*, 45(3):221–229.
- Friedman, I., Benson, C., and Gleason, J. (1991). Isotopic changes during snow metamorphism. *Stable Isotope Geochemistry: A Tribute to Samuel Epstein*, (3):211–221.
- Gat, J. R. (2010). *Isotope hydrology: A study of the hydrologic cycle*. Imperial College Press.
- Grootes, P., Stuiver, M., Thompson, L., and Mosley-Thompson, E. (1989). Oxygen isotope changes in tropical ice, Quelccaya, Peru. *Journal of Geophysical Research*, 94(D1):1187–1194.
- Higgins, J. A., Kurbatov, A. V., Spaulding, N. E., Brook, E., Introne, D. S., Chimiak, L. M., Yan, Y., Mayewski, P. A., and Bender, M. L. (2015). Atmospheric composition 1 million years ago from blue ice in the Allan Hills, Antarctica. *Proceedings of the National Academy of Sciences*, 112(22):6887–6891.
- Hoshina, Y., Fujita, K., Nakazawa, F., Iizuka, Y., Miyake, T., Hirabayashi, M., Kuramoto, T., Fujita, S., and Motoyama, H. (2014). Effect of accumulation rate on water stable isotopes of near-surface snow in inland Antarctica. *Journal of Geophysical Research Atmospheres*, 119:274–283.
- Johnsen, S. J., Clausen, H. B., Cuffey, K. M., Hoffmann, G., Schwander, J., and Creyts, T. (2000). Diffusion of stable isotopes in polar firn and ice: the isotope effect in firn diffusion. In Hondoh, T., editor, *Physics of Ice Core Records*, pages 121 – 150. Hokkaido University Press, Sapporo.
- Jouzel, J., Alley, R. B., Cuffey, K. M., Dansgaard, W., Hoffmann, P. G. G., Koster, R. D., Peel, D., Shuman, C. A., Stievenard, M., and Tm, J. W. (1997). Validity of the temperature reconstruction from water isotopes in ice cores. 102(97):26471 – 26487.
- Kim, K. and Lee, X. (2011). Isotopic enrichment of liquid water during evaporation from water surfaces. *Journal of Hydrology*, 399(3-4):364–375.
- Lacelle, D. (2011). On the ^{18}O , D and D-excess relations in meteoric precipitation and during equilibrium freezing: Theoretical approach and field examples. *Permafrost and Periglacial Processes*, 22(1):13–25.
- Lacelle, D., Davila, A. F., Fisher, D., Pollard, W. H., Dewitt, R., Heldmann, J., Marinova, M. M., and Mckay, C. P. (2013). Excess ground ice of condensation-diffusion origin in University Valley, Dry Valleys of Antarctica: Evidence from isotope geochemistry and numerical modeling. *Geochimica et Cosmochimica Acta*, 120:280–297.

- Lacelle, D., Davila, A. F., Pollard, W. H., Andersen, D., Heldmann, J., Marinova, M., and McKay, C. P. (2011). Stability of massive ground ice bodies in University Valley, McMurdo Dry Valleys of Antarctica: Using stable OH isotope as tracers of sublimation in hyper-arid regions. *Earth and Planetary Science Letters*, 301(1-2):403–411.
- Lamp, J. L. and Marchant, D. R. (2017). Vapor transport and sublimation on Mullins Glacier, Antarctica. *Earth and Planetary Science Letters*, 465:82–91.
- Lécuyer, C., Royer, A., Fourel, F., Seris, M., Simon, L., and Robert, F. (2017). D/H fractionation during the sublimation of water ice. *Icarus*, 285(December 2016):1–7.
- Lehmann, M. and Siegenthaler, U. (1991). Equilibrium oxygen-and hydrogen-isotope fractionation between ice and water. *Journal of Glaciology*, (125):23–26.
- Lorius, C., Merlivat, L., Jouzel, J., and Pourchet, M. (1979). A 30,000-yr isotope climatic record from Antarctic ice. *Nature*, 280(5724):644–648.
- Machida, T., Nakazawa, T., Narita, H., Fujii, Y., Aoki, S., and Watanabe, O. W. (1996). Variations of the CO₂, CH₄, and N₂O concentrations and ¹³C of CO₂ in the glacial period deduced from an Antarctic ice core, South Yamato. In *Proceedings of the NIPR Symposium of Polar Meteorology and Glaciology*, pages 55–65.
- Mader, H. M. (1992). Observations of the water-vein system in polycrystalline ice. *Journal of Glaciology*, 38(130):333–347.
- Marchant, D. R. and Head, J. W. (2007). Antarctic dry valleys: Microclimate zonation, variable geomorphic processes, and implications for assessing climate change on Mars. *Icarus*, 192(1):187–222.
- Matsuoka, K. (1999). Mass Balance Features Derived from a Firn Core at Hielo Patagónico Norte, South America. *Arctic, Antarctic, and Alpine Research*, 31(4):333–340.
- Merlivat, L. and Jouzel, J. (1979). Global climatic interpretation of the deuterium-oxygen 18 relationship for precipitation. *Journal of Geophysical Research*, 84(C8):5029–5033.
- Merlivat, L. and Nief, G. (1967). Fractionnement isotopique lors des changements d'état solide-vapeur et liquide-vapeur de l'eau à des températures inférieures à 0C. *Tellus*, 19(1):122–127.
- Morgan, V., Wookey, C., Li, J., van Ommen, T., Skinner, W., and Fitzpatrick, M. (1997). Site information and initial results from TI . deep ice drilling on Law Dome, Antarctica. *Journal of Glaciology*, 43(143):3–10.
- Muggeo, V. M. R. (2003). Estimating regression models with unknown break-points. *Statistics in Medicine*, 22(19):3055–3071.

- Muggeo, V. M. R. (2008). segmented: An R package to Fit Regression Models with Broken-Line Relationships. *R News*, 8(May):20–25.
- Nasello, O. B., Navarro de Juarez, S., and Di Prinzio, C. L. (2007). Measurement of self-diffusion on ice surface. *Scripta Materialia*, 56(12):1071–1073.
- Nestlé Waters North America (2016). Poland Spring bottled water quality report. Technical report, Nestle Waters North America, Inc.
- Neumann, T. A., Albert, M. R., Engel, C., Courville, Z., and Perron, F. (2009). Sublimation rate and the mass-transfer coefficient for snow sublimation. *International Journal of Heat and Mass Transfer*, 52(1-2):309–315.
- Nye, J. F. (1998). Diffusion of isotopes in the annual layers of ice sheets. *Journal of Glaciology*, 44(148):467–468.
- O’Neil, J. R. (1968). Hydrogen and oxygen isotope fractionation between ice and water. *Journal of Physical Chemistry*, 72(10):3683–3684.
- Ramseier, R. O. (1967). Self-Diffusion of Tritium in Natural and Synthetic Ice Monocrystals. *Journal of Applied Physics*, 38(6):2553 – 2556.
- Rempel, A. W., Waddington, E. D., Wettlaufer, J. S., and Worster, M. G. (2001). Possible displacement of the climate signal in ancient ice by premelting and anomalous diffusion. *Nature*, 411(6837):568–571.
- Schotterer, U., Stichler, W., and Ginot, P. (2004). The Influence of Post-Depositional Effects on Ice Core Studies: Examples From the Alps, Andes, and Altai. In *Earth Paleoenvironments: Records Preserved in Mid- and Low-Latitude Glaciers*, number 2004, pages 39–59.
- Sokratov, S. A. and Golubev, V. N. (2009). Snow isotopic content change by sublimation. *Journal of Glaciology*, 55(193):823–828.
- Souchez, R. and Jouzel, J. (1984). On the isotopic composition in D and ^{18}O of water and ice during freezing. *Journal of Glaciology*, 30(106):369–372.
- Spaulding, N. E., Higgins, J. A., Kurbatov, A. V., Bender, M. L., Arcone, S. A., Campbell, S., Dunbar, N. W., Chimiak, L. M., Introne, D. S., and Mayewski, P. A. (2013). Climate archives from 90 to 250ka in horizontal and vertical ice cores from the allan hills blue ice area, antarctica. *Quaternary Research (United States)*, 80(3):562–574.
- Stichler, W. and Schotterer, U. (2000). From accumulation to discharge: Modification of stable isotopes during glacial and post-glacial processes. In *Hydrological Processes*, volume 14, pages 1423–1438.

- Stichler, W., Schotterer, U., Fröhlich, K., Ginot, P., Kull, C., Gäggeler, H., and Pouyaud, B. (2001). Influence of sublimation on stable isotope records recovered from high-altitude glaciers in the tropical Andes. *Journal of Geophysical Research*, 106(D19):22613.
- Town, M. S., Warren, S. G., Walden, V. P., and Waddington, E. D. (2008). Effect of atmospheric water vapor on modification of stable isotopes in near-surface snow on ice sheets. 113(August):1–16.
- Uyeda, H. and Kikuchi, K. (1978). Freezing Experiment of Supercooled Water Droplets by Using Single Crystal Ice. *Journal of the Meteorological Society of Japan*, 56(1):43–51.
- Winter, K., Woodward, J., Dunning, S. A., Turney, C. S., Fogwill, C. J., Hein, A. S., Gолledge, N. R., Bingham, R. G., Marrero, S. M., Sugden, D. E., and Ross, N. (2016). Assessing the continuity of the blue ice climate record at Patriot Hills, Horseshoe Valley, West Antarctica. *Geophysical Research Letters*, 43(5):2019–2026.

CURRICULUM VITAE

